Geomechanics and Engineering, *Vol. 30, No. 3 (2022) 273-280*
https://doi.org/10.12989/gae.2022.30.3.273

Vertical Z-vibration prediction model of ground building induced by subway operation

Binghua Zhou[1], Yiguo Xue*[1], Jun Zhang[2], Dunfu Zhang[1], Jian Huang[2], Daohong Qiu[1], Lin Yang[2], Kai Zhang[1] and Jiuhua Cui[1]

[1]*Geotechnical and Structural Engineering Research Center, Shandong University, Ji'nan 250061, Shandong, China*
[2]*Qingdao Metro Group Co. Ltd., Qingdao 266000, Shandong, China*

(*Received August 7, 2020, Revised May 17, 2022, Accepted July 12, 2022*)

Abstract. A certain amount of random vibration excitation to subway track is caused by subway operation. This excitation is transmitted through track foundation, tunnel, soil medium, and ground building to the ground and ground structure, causing vibration. The vibration affects ground building. In this study, the results of ANSYS numerical simulation was used to establish back-propagation (BP) neural network model. Moreover, a back-propagation neural network model consisting of five input neurons, one hidden layer, 11 hidden-layer neurons, and three output neurons was used to analyze and calculate the vertical Z-vibration level of New Capital's ground buildings of Qingdao Metro phase I Project (Line M3). The Z-vibration level under different working conditions was calculated from monolithic roadbed, steel-spring floating slab roadbed, and rubber-pad floating slab roadbed under the working condition of center point of 0-100 m. The steel-spring floating slab roadbed was used in the New Capital area to monitor the subway operation vibration in this area. Comparing the monitoring and prediction results, it was found that the prediction results have a good linear relationship with lower error. The research results have good reference and guiding significance for predicting vibration caused by subway operation.

Keywords: ground building; neural network; vibration induced by subway operation; Z-vibration

1. Introduction

A large number of subways were built to solve traffic problems in big cities around the world. People can enjoy the convenience of subway rail transport. However, the environmental vibration and noise problems caused by subway operation are neglect. As shown in Fig. 1, when a train is running in the subway, the upper buildings or inhabitants are affected by the surface vibration and noise caused by the train, and the residents and equipment in the buildings receive secondary vibration and secondary noise (Zapfe and Ungar 2000).

The impact of subway trains on the vibration and noise of the surrounding environment has aroused wide public concern. The vibration and noise of subway trains have been widely studied, and good results were achieved. Xue *et al*. (2014) found that the vibration waves of different characteristics attenuate according to different regularities in the rock layer due to the existence of geometric and material damping. In addition, the effects of basic reaction amplitude frequency characteristic curve and ballast bed material on the vibration characteristics of a rail bed structure and the coupling system of the rail bed of the steel plate were analyzed. Haghnejad *et al*. (2018) considered geological discontinuities to investigate the effect of ground vibration. Degrande *et al*. (2004) established a finite-element boundary element model of building vibration induced by a rail transit according to the interactions of soil structure. Connolly *et al*. (2013) also used the finite-element boundary-element method to establish a three-dimensional numerical model of the vibration of a multilayer frame structure caused by a ground train. Takemiya (2003) established a simulation model of Swedish Ledsgard high-speed train track and used the model to predict the ground vibration caused by train. Zhang *et al*. (2011) used an approximate relationship to represent the propagation of ground vibration caused by a dynamic surface source as a function of distance, wave area, geometric attenuation coefficient, and soil attenuation coefficient. Ali *et al*. (2005) studied the law of noise propagation in buildings along a subway through field measurements and established a physical model of the building. Nagy *et al*. (2006) proposed a new method for predicting the secondary noise of an indoor structure based on the overall Rayleigh wave and direct boundary element method. With *et al*. (2006) proposed a semi-empirical prediction model based on the Swedish Ministry of Railways forecast projects on railway vibration by test data and theoretical analysis. Hou *et al*. (2016) verified the correctness of the structure vibration predicted by a numerical model of the spatially coupled vehicle–track–building system. The dynamic responses to train-track-railway station are computed using finite-element analysis in conjunction with the adaptation of (analytical) system coupling techniques by Zhu *et al*. (2017). Fatahi *et al*. (2014) have undertook inelastic dynamic analysis under the influence of four different earthquake ground motions. Majumder *et al*. (2017) used

*Corresponding author, Professor
E-mail: xieagle@sdu.edu.cn

ISSN: 2005-307X (Print), 2092-6219 (Online)

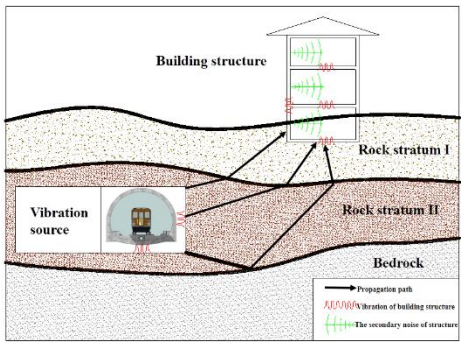

Fig. 1 Environmental vibration caused by the subway system (Zou *et al*. 2020)

vertically oscillated strip foundation as the vibration source intermittent geofoam to assess the efficiency of the vibration screening technique.

These studies focused on the propagation and attenuation of vibrating waves caused by subway operations in rock formation and measured vibration reduction under different working conditions; however, a nonlinear prediction model of environmental vibration under different track types with rock formation characteristics has been rarely developed. The vibration problem caused by subway operation is very complex and a nonlinear solution problem. The traditional empirical model and numerical simulation method have certain limitations. However, in artificial neural network, many hidden-layer networks have excellent feature learning ability, and network training can be solved by "layer-by-layer initialization" and "reverse fine-tuning" technology (Cevik *et al*. 2011, Hinton *et al*. 2006, Arel *et al*. 2010). Neural networks have been widely used in geotechnical engineering (Luat *et al*. 2020, Koopialipoor *et al*. 2020). It is possible to accurately solve complex subway vibration problems. Therefore, based on the propagation and attenuation characteristics of train vibration waves in different strata, it is very important to study a nonlinear prediction model of subway vibration load on ground floor using a back-propagation (BP) neural network.

2. BP neural network model

A BP neural network is a feedback type fully connected multilayer neural network. It has strong associative memory and generalization ability (Hornik *et al*. 1989, Funahashi *et al*. 1989). a standard BP neural network model is made up of three layers of neurons: input layer, hidden layer, and output layer. The hidden layer of network topology can be multilayer. For the input neuron of the BP model, its input and output are the same, i.e., O_j=X_j. The neurons in the intermediate and output layers satisfy Eq. (1).

$$O_j = f_j(Net_j) = f_j(\sum W_j X_j + \theta_j) \quad (1)$$

where f_j is the excitation function corresponding to neuron *j*. At present, the most used excitation function is the Sigmoid function: $f(x) = \frac{1}{1+e^{-x}}$. θ_j is the threshold of neuronal *j*. X_j is the input to the neuronal *j*. W_j is the corresponding input and the connection weight of neuron *j*.

The storage information of a BP network has mainly two aspects. On one hand, it is the architecture of the network, i.e., the number of nodes in the network input layer, hidden layer, and output layer. On the other hand, it is the connection weight among the adjacent-layer nodes. The main parameters influencing the network structure is the number of hidden layer, learning rate, and system error in the hidden layer. The number of nodes in the input and output layers is determined by the application of the system. The number of hidden-layer nodes is determined by the user. If the number is too small, it will affect the effectiveness of the network. If the number is too much, it will significantly increase the time of network training. The learning rate is usually between 0.1 and 0.9. In general, a smaller learning rate can lead to a higher number of training sessions. If the learning rate too much, it will affect the stability of the network structure. The system error is usually determined by the output requirements. The lower system error, the higher the accuracy.

The specific steps of a BP neural-network algorithm can be summarized as follows.

a) The input vector *X* and target output vector *T* are given, and the network weights are initialized.
b) Calculate the actual output of the network.
c) Calculate the error between the actual output vector of the network and the required output of the target.
d) Weight learning makes the error minimum.

3. Construction of learning samples

The establishment of a BP neural network model requires a convincing data learning sample set. It is much difficult to obtain the Z-vibration level of a ground building under different conditions. In this study, numerical simulation was used to introduce enough parameter samples to construct the best artificial neural network model.

3.1 Engineering situation

Qingdao Metro (Line M3) is a rail transit backbone connecting the North and South (Fig. 2). It is positioned as a large-capacity line, serving both the central district of the central city and outlying fringe groups. It also has the function of traffic easing and guiding development. It is about 24.9 km in length, mostly in ground down. There are 22 stations including 6 transfer stations with an average distance of 1.165 km. There is a road depot and an integrated base, located near the end of the line in Qingdao North Station, and there is a control center, located at the northeast corner of Nanjing road and West Liaoyang Road intersection. The surface rock is quaternary rock. The underlying rock is mainly Yanshanian granite. The subway tunnel passes through the weathered and slightly weathered rock mass. Some areas are rich in groundwater, and even appear drift sand stratum.

3.2 Determination of finite-element dynamic model for subway operation

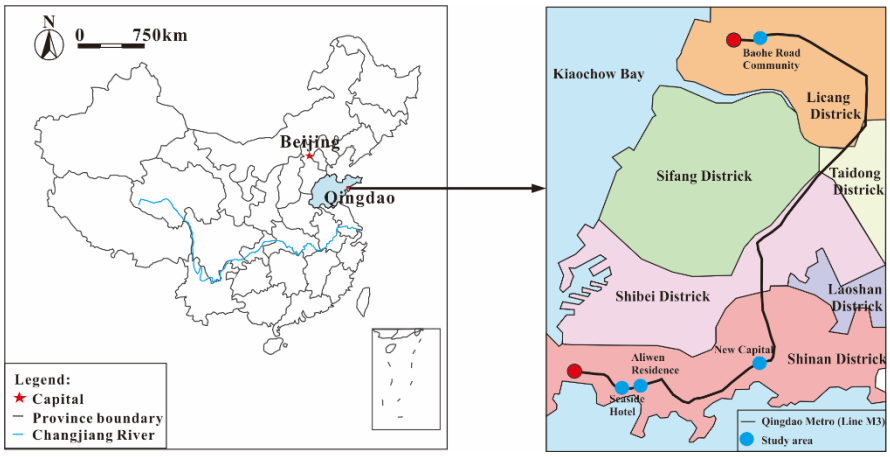

Fig. 2 Location map of Qingdao Metro (Line M3)

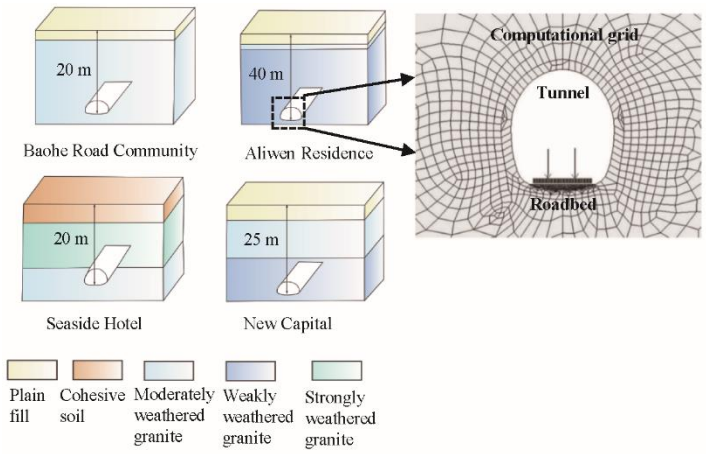

Fig. 3 Computational model diagram

Table 1 Parameters of numerical simulation model

Model size (m)	Number of calculation unit	Tunnel unit size(m)	Roadbed unit size(m)	Surface unit size(m)	Other unit size(m)
240×60	8349	0.05×0.05	0.05×0.05	0.5×0.5	1×1

In this paper, many numerical analyses were used to predict the *Z*-vibration level of ground buildings induced by subway operation.

The following simplifications and assumptions were made:

a) The soil medium is an infinite elastic layer.

b) The properties of each layer are the same, homogeneous and isotropic. Different soil layers have different properties. The interface satisfies compatibility condition under the dynamic action. There is no detachment and relative sliding between the soil layers.

c) The model is a planar strain model.

d) The total stress method can be used for calculation.

The tunnel in Qingdao Metro (Line M3) is horse-shoe shaped. The maximum span of the tunnel is 5.54 m, and the height of the tunnel is 5.45 m. The lining thickness is 0.45 m. The lining material is C30 concrete. According to the formation conditions, the specific parameters of the model are shown in Table 1. The numerical model figure is shown in Fig. 3.

3.3 Numerical calculation results

Baohe Road Community area, Aliwen Residence area, and the former site of Seaside Hotel area near Qingdao Metro (Line M3) were taken as an example. The mileage of Baohe Road Community area is K23+565 to K23+795 which are mainly composed of plain fill and a moderately weathered granite layer. The mileage of Aliwen Residence area is K2+220 to K2+335 which are mainly composed of plain fill, a moderately weathered granite layer, and weakly weathered granite. The mileage of the former site of Seaside Hotel area is K2+555 to K2+655.which are mainly composed of cohesive soil, a strongly weathered granite layer, and a moderately weathered granite layer. According to the geological profile, the distribution of each stratum and average buried depth were obtained as shown in Fig. 3. The duration excitation load was applied to their finite-element model. A transient analysis was performed using the finite-element analysis software. The Z-vibration level for different points under different roadbeds which consider the track irregularity to establish the motion equation of the structure was calculated (Fig. 4). The numerical simulation data are shown in Table 2.

Fig. 4(a) shows that the maximum Z-vibration level is 78 dB in the monolithic roadbed of Baohe Road community. It appears at about 10 m away from the tunnel,

Table 2 Parameters of numerical simulation model

	Baohe Road Community area			Aliwen Residence area			Seaside Hotel area		
	Monolithic roadbed (dB)	Steel-spring floating slab roadbed (dB)	Rubber-pad floating slab roadbed (dB)	Monolithic roadbed (dB)	Steel-spring floating slab roadbed (dB)	Rubber-pad floating slab roadbed (dB)	Monolithic roadbed (dB)	Steel-spring floating slab roadbed (dB)	Rubber-pad floating slab roadbed (dB)
1	78	69.8	70.2	80	66	62	77.8	62	59
2	74.8	66	66.5	78	65.2	60.8	77	61	58.6
3	70.9	62.9	62.9	75	62	57	72	56	53.8
4	69.8	62.6	61.7	72	59	54	69.2	51.8	50
5	69	62	61.1	69.6	55	51	67	46.4	46
6	67	59.8	59.1	66.2	52	48.2	63	41.2	43

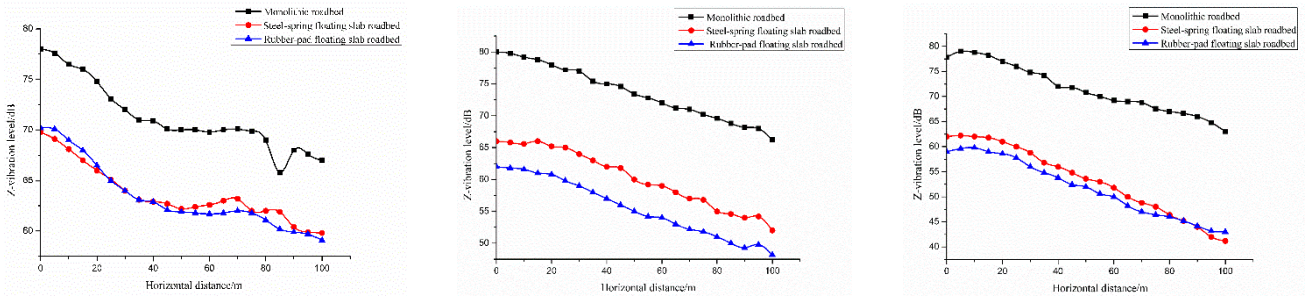

(a) Baohe Road Community (b) Aliwen Residence (c) Seaside Hotel

Fig. 4 Z-vibration level with horizontal distance

and the Z-vibration level decreases with the increase in the horizontal distance beyond 10 m. The variation trend of Z-vibration level along the horizontal distance between steel-spring floating slab roadbed and rubber-pad floating slab roadbed is similar to that of the horizontal distance of Z-vibration level under the monolithic roadbed. The maximum Z-vibration level of steel-spring floating slab roadbed is 69.8 dB, and the maximum Z-vibration level of rubber-pad floating slab roadbed is 70.2 dB.

Fig. 4(b) shows that the maximum Z-vibration level in the monolithic roadbed of Baohe Road Community area is 80 dB. It appears at about 10 m away from the tunnel, and the Z-vibration level decreases with the increase in the horizontal distance beyond 10 m. The trend of Z-vibration level along the horizontal distance between steel-spring floating slab roadbed and rubber-pad floating slab roadbed is similar to that of the horizontal distance of Z-vibration level under a monolithic roadbed. The maximum Z-vibration level of steel-spring floating slab roadbed is 66 dB, and the maximum Z-vibration level of rubber-pad floating slab roadbed is 62 dB.

Fig. 4(c) shows that the maximum Z-vibration level in the monolithic roadbed of Seaside Hotel area is 78 dB. It appears at about 10 m away from the tunnel, and the Z-vibration level decreases with the increase in the horizontal distance beyond 10 m. The trend of Z-vibration level along the horizontal distance between steel-spring floating slab roadbed and rubber-pad floating slab roadbed is similar to that of the horizontal distance of Z-vibration level under a monolithic roadbed. The maximum Z-vibration level of steel-spring floating slab roadbed is 62 dB, and the maximum Z-vibration level of rubber-pad floating slab roadbed is 59 dB.

3.4 Constructing BP neural network learning samples

The sample of BP neural network must be representative and uniform; therefore, the learning sample set was constructed as shown in Table 3. There are five neurons in the input layer such as the distance from the center point, depth of the tunnel, elastic modulus of the stratum, Poisson's ratio of the rock stratum, and density of the rock stratum. The output layer selected three neurons which corresponding to the Z-vibration level of each point under the monolithic roadbed, Z-vibration level of each point under the steel-spring floating slab roadbed, and Z-vibration level of each point under the rubber-pad floating slab roadbed.

3.5 Input model of BP neural network

After obtaining the sample set, the three-layer BP network was used for learning. The input and output raw data were converted into valid numeric data. The input vector X was obtained from the distance from the center, buried depth of the tunnel, elastic modulus of rock stratum, Poisson's ratio, and rock density. The output vector Y consists of Z-vibration level under monolithic roadbed, Z-vibration level under steel-spring floating slab roadbed, and Z-vibration level under rubber-pad floating slab roadbed. As shown in Table 4, an implicit layer was set up. After repeated debugging, the convergence of the network was better when the number of nodes in the hidden layer was n=11 and the learning accuracy was 0.01, which can be used for inversion calculation. At the same time, each sample is input into the network for learning, and the mean square error of the output became stable after 5,000

Table 3 Neural network learning sample of the Z-vibration level of ground building influenced by subway vibration load

	Input					Desired output		
	The distance from the center point (m)	The depth of the tunnel (m)	The elastic modulus (MPa)	Poisson's ratio	Density (kg/m^3)	Z -vibration level of monolithic roadbed (dB)	Z-vibration level of steel-spring floating slab roadbed (dB)	Z-vibration level of rubber-pad floating slab roadbed (dB)
1	0	20	4694	0.26	2407	78	69.8	70.2
2	20	20	4694	0.26	2407	74.8	66	66.5
3	40	20	4694	0.26	2407	70.9	62.9	62.9
4	60	20	4694	0.26	2407	69.8	62.6	61.7
5	80	20	4694	0.26	2407	69	62	61.1
6	100	20	4694	0.26	2407	67	59.8	59.1
7	0	40	17426	0.26	2345	80	66	62
8	20	40	17426	0.26	2345	78	65.2	60.8
9	40	40	17426	0.26	2345	75	62	57
10	60	40	17426	0.26	2345	72	59	54
11	80	40	17426	0.26	2345	69.6	55	51
12	100	40	17426	0.26	2345	66.2	52	48.2
13	0	25	6315	0.25	2384	77.8	62	59
14	20	25	6315	0.25	2384	77	61	58.6
15	40	25	6315	0.25	2384	72	56	53.8
16	60	25	6315	0.25	2384	69.2	51.8	50
17	80	25	6315	0.25	2384	67	46.4	46
18	100	25	6315	0.25	2384	63	41.2	43

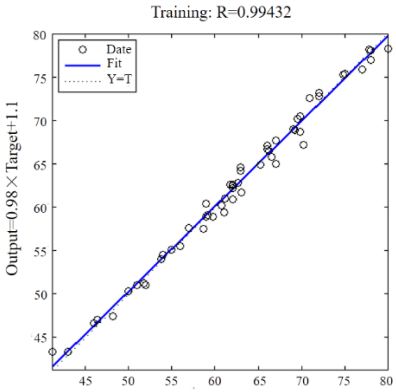

Fig. 5 Correlation coefficient of model

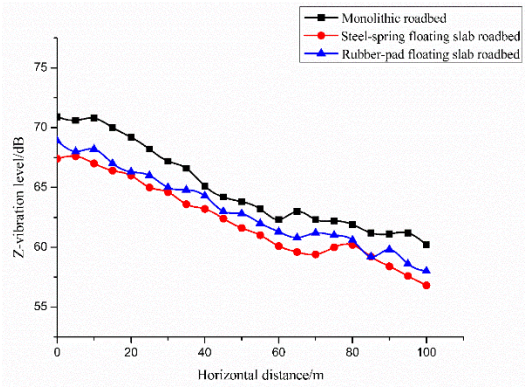

Fig. 6 Z-vibration level with horizontal distance in New Capital area

Table 4 Optimal BP neural network model information

Number of input neurons	Number of output neurons	Number of hidden layers	Number of neurons in the hidden layer	Target error	Epochs	Learning accuracy
5	3	1	11	0.001	5000	0.01

Table 5 Physical and mechanical parameters of the rock layer

Elastic modulus (MPa)	Density (kg/ m^3)	Poisson's ratio
12881	2410	0.26

iterations. The correlation coefficient of the optimal neural network model is shown in Fig. 5.

4. Back analysis of BP neural network model

4.1 Selection of the study object

According to the information of Qingdao Metro (Line M3), New Capital area was selected to study the impact of Z-vibration level on ground buildings. The mileage of New Capital area is K7+500 to K8+020. In this channel section, the strata are mainly composed of plain fill, a moderately weathered lamprophyre layer, and weakly weathered granite. Specific engineering geology and buried depth are shown in Fig. 3. The physical and mechanical parameters of the rock layer are shown in Table 5.

4.2 Prediction of Z-vibration level for New Capital area based on numerical simulation

This section is basically the same as numerical simulation in the third chapter of this paper. The Z-vibration level of ground buildings under different roadbed forms was

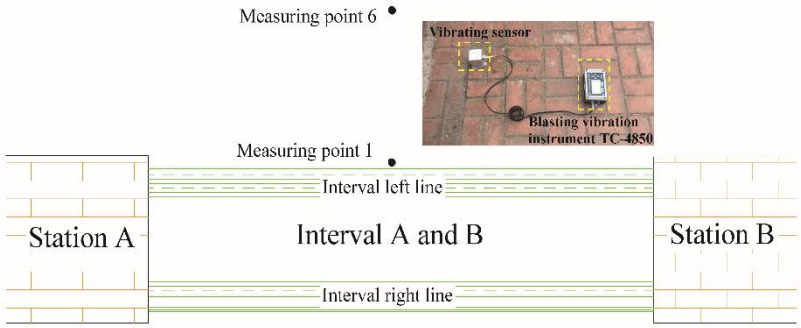

Fig. 7 Layout of measuring points

Table 7 Input parameters of BP neural network model

	Distance from the center point (m)	Depth of the tunnel (m)	Elastic modulus (MPa)	Poisson 's ratio	Density (kg/m^3)
1	0	25	12881	0.26	2410
2	20	25	12881	0.26	2410
3	40	25	12881	0.26	2410
4	60	25	12881	0.26	2410
5	80	25	12881	0.26	2410
6	100	25	12881	0.26	2410

obtained by numerical simulation, as shown in Fig. 6. The data are shown in Table 6.

Fig. 7 shows that the maximum Z-vibration level is 70.9 dB in the monolithic roadbed of New Capital area. It appears at about 10 m away from the tunnel, and the Z-vibration level decreases with the increase in the horizontal distance beyond 10 m. The trend of Z-vibration level along the horizontal distance between steel-spring floating slab roadbed and rubber-pad floating slab roadbed is similar to that of the horizontal distance of Z-vibration level under the monolithic roadbed. The maximum Z-vibration level of steel-spring floating slab roadbed is 67.4 dB, and the maximum Z-vibration level of rubber-pad floating slab roadbed is 68.9 dB.

4.3 Prediction of Z-vibration level for New Capital area based on BP neural network

The BP neural network model established above was used, and the valid input parameters in Table 7 were put in the BP neural network model. As shown in Table 8, the Z-vibration level of the ground building with the horizontal distance was obtained for New Capital area.

4.4 Field monitoring on subway operation

The test site is the New Capital area of Qingdao Metro phase I Project (line 3). The track roadbed in the region is made of a steel-spring floating slab roadbed. The test had six measuring points. The measuring points were selected within the range of 100 m in each region, and a measuring point was laid every 20 m. A blasting vibration instrument TC-4850 was used to collect the data in the field. The layout of measuring points is shown in Fig. 7.

From the vibration monitoring results of the new area, it

Table 8 BP neural network results of the Z-vibration level of ground buildings under different working conditions in New Capital area

	Distance from the center point (m)	Monolithic roadbed (dB)	Steel-spring floating slab roadbed (dB)	Rubber-pad floating slab roadbed (dB)
1	0	70.6	66.9	68
2	20	69.7	66.2	67.3
3	40	65.7	63.5	65.1
4	60	62.5	60.8	62
5	80	61.3	58.9	61.3
6	100	59.8	56.2	59

Table 9 Parameters of numerical simulation model

Distance from the center point (m)	Z-vibration level (dB)
0	66
20	65
40	63.2
60	60.6
80	59.8
100	57.3

can be concluded that the maximum Z-vibration level is 66 dB. The monitoring data are shown in Table 9.

4.5 Error analysis

Good or bad can be evaluated in many ways. The main methods are Mean Absolute Deviation (MAD), Mean Square Error (MSE), Mean Absolute Percentage Error (MAPE), and Mean Percentage Error (MPE). If $\hat{y}_i$ is the predicted value and y_i is the actual value, the error of measured calculation formula are as follows from Eqs. (2) to (5)

$$MAD = \frac{1}{n}\sum_{i=1}^{n}|y_i - \hat{y}_i| \tag{2}$$

$$MSE = \frac{1}{n}\sum_{i=1}^{n}(y_i - \hat{y}_i)^2 \tag{3}$$

$$MAPE = \frac{1}{n}\sum_{i=1}^{n}\frac{|y_i - \hat{y}_i|}{y_i} \tag{4}$$

$$MPE = \frac{1}{n}\sum_{i=1}^{n}\frac{(y_i - \hat{y}_i)}{y_i} \tag{5}$$

The calculation results of different prediction methods are shown in Table 10, and the performance indices of

Table 10 Calculation results of different prediction methods

Distance from the center point (m)	Numerical simulation results (dB)	BP neural network results (dB)	Monitoring data (dB)
0	67.4	66.9	66
20	66	66.2	65
40	63.2	63.5	63.2
60	60.1	60.8	60.6
80	60.2	58.9	59.8
100	56.8	56.2	57.3

Table 11 Performance indices of different forecasting methods

Prediction method	MAD	MSE	MAPE	MPE
Numerical simulation	0.633	0.603	0.010	-0.004
BP neural network	0.8	0.733	0.012	-0.006

different forecasting methods are shown in Table 11.

Fig. 8 shows a good linear relationship between the predicted results of the two methods and the actual measured values, and Table11 shows that MAD and MSE are slightly larger. Considering the complexity and uncontrollable nature of actual engineering conditions, the predicted results are more accurate.

5. Discussion

Many factors affect the vibration of subway, and the vibration mechanism is complex. The numerical simulation method used in this study failed to make a thorough and systematic study of various influencing factors. It is necessary to establish a dynamic finite-element model of the train track and subgrade soil structure of a metro depot according to the subway line, ground, and building above the subway; the influence of subgrade, track, vehicle, structure, and other factors on the vibration response of surface buildings can be further studied. It provides a more effective reference for the Z-vibration level prediction model of vertical vibration caused by subway.

A BP neural network severely depends on the diversity of training samples. The training samples are diversified, and the training accuracy is higher. In this paper, the training samples are not comprehensive; in the future, through the sharing of resources, large data processing, and multidisciplinary cooperation, more comprehensive and reliable ground vibration for Z-vibration level data can be selected, and diverse Z-vibration level prediction models can be developed.

6. Conclusions

A BP neural network has good nonlinear information storage ability and adaptability. A BP neural network can be used to determine the Z-vibration level of ground buildings by subway operation. It can provide a reference for the calculation of the project and has practical significance for the evaluation of the subway track form and information design.

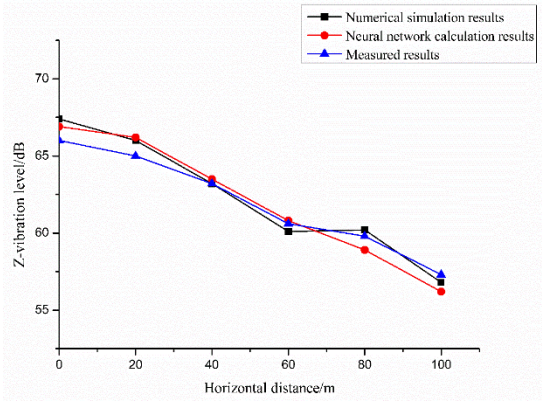

Fig. 8 Data comparison

The influencing factors of Z-vibration level for ground buildings include the distance from the center, buried depth of the tunnel, elastic modulus of rock stratum, Poisson's ratio, and rock density. The BP neural network structure for predicting the Z-vibration level of ground buildings included five input neurons, one hidden layer, 11 hidden-layer neurons, and three output neurons.

In this study, a BP neural network learning sample established to calculate the Z-vibration level of ground buildings in New Capital area. Comparing the monitoring and prediction results, it was found that the prediction results have a good linear relationship with lower error. This can satisfy the engineering requirements and further proves that the artificial neural network has good performance in predicting the vertical Z-vibration level of ground buildings under subway operation.

Acknowledgments

Much of the work presented in this paper was supported by the National Natural Science Foundations of China (grant numbers 41877239, 51379112, 51422904 and 41772298), and the State Key Development Program for Basic Research of China (grant number 2013CB036002), and the Fundamental Research Funds of Shandong University (grant number 2018JC044), and Shandong Provincial Natural Science Foundation (grant number JQ201513). The authors would like to express appreciation to the reviewers for their valuable comments and suggestions that helped improve the quality of our paper.

References

Ali, S.A. (2005), "Railway noise levels, annoyance and countermeasures in Assiut, Egypt", *Appl. Acoust.*, **66**(1), 105-113. https://doi.org/10.1016/j.apacoust.2004.06.005.

Arel, I., Rose, D.C. and Karnowski, T.P. (2010), "Research frontier: Deep machine learning-a new frontier in artificial intelligence research", *IEEE Comput. Intell. Mag.*, **5**(4), 13-18. https://doi.org/10.1109/MCI.2010.938364.

Cevik, A., Sezer, E.A., Cabalar, A.F. and Gokceoglu, C. (2011),

"Modeling of the uniaxial compressive strength of some clay-bearing rocks using neural network", *Appl. Soft. Comput*., **11**(2), 2587-2594. https://doi.org/10.1016/j.asoc.2010.10.008.

Connolly, D., Giannopoulos, A. and Forde, M.C. (2013), "Numerical modelling of ground borne vibrations from high speed rail lines on embankments", *Soil Dyn. Earthq. Eng*., **46**(1), 13-19. https://doi.org/10.1016/j.soildyn.2012.12.003.

Fatahi, B., Tabatabaiefar, S.H.R. and Samali, B. (2014), "Soil-structure interaction vs Site effect for seismic design of tall buildings on soft soil", *Geomech. Eng*., **6**(3), 293-320. https://doi.org/10.12989/gae.2014.6.3.293.

Funahashi, K. (1989), "On the approximate realization of continuous mappings by neural networks", *Neur. Network*., **2**(3), 183-192. https://doi.org/10.1016/0893-6080(89)90003-8.

Haghnejad, A., Ahangari, K., Moarefvand, P. and Goshtasbi, K. (2018), "Numerical investigation of the impac of geological discontinuities on the propagation of ground vibrations", *Geomech. Eng*., **14**(6), 545-552. https://doi.org/10.12989/gae.2018.14.6.545.

Hinton, G.E. and Salakhutdinov, R.R. (2006), "Reducing the dimensionality of data with neural networks", *Sci.*, **313**(5786), 504-507. https://doi.org/10.1126/science.1127647.

Hornik, K., Stinchcombe, M. and White, H. (1989), "Multilayer feedforward networks are universal approximators", *Neur. Network*., **2**(5), 359-366. https://doi.org/10.1016/0893-6080(89)90020-8.

Hou, B., Gao, L., Xin, T. and Cai, X. (2016), "Prediction of structural vibrations using a coupled vehicle-track–building model", *Proc. Inst. Mech. Eng. Part F-J. Rail Rapid Transit*., **230**(2), 510-530. https://doi.org/10.1177/0954409714548244.

Koopialipoor, M., Fahimifar, A., Ghaleini, E.N., Momenzadeh, M. and Armaghani, D.J. (2020), "Development of a new hybrid ANN for solving a geotechnical problem related to tunnel boring machine performance", *Eng. Comput*., **36**(1), 345-357. https://doi.org/10.1007/s00366-019-00701-8.

Luat, N.V., Lee, K. and Thai, D.K. (2020), "Application of artificial neural networks in settlement prediction of shallow foundations on sandy soils", *Geomech. Eng*., **20**(5), 385-397. https://doi.org/10.12989/gae.2020.20.5.385.

Majumder, M., Ghosh, P. and Sathiyamoorthy, R. (2017), "An innovative vibration barrier by intermittent geofoam-A numerical study", *Geomech. Eng*., **13**(2), 269-284. https://doi.org/10.12989/gae.2017.13.2.269.

Nagy, A.B., Fiala, P., Márki, F., Augusztinovicz, F., Degrande, G. and Jacobs, S. (2006), "Prediction of interior noise in buildings generated by underground rail traffic", *J. Sound Vib*., **293**(3), 680-690. https://doi.org/10.1016/j.jsv.2005.12.011.

Pyl, L., Lombaert, G., Haegeman, W. and Degrande, G. (2004), "Validation of a source–receiver model for road traffic-induced vibrations in buildings I: Source model", *J. Eng. Mech*., **46**(1), 1377-1393. https://doi.org/10.1061/(ASCE)0733-9399(2004)130:12(1377).

Takemiya, H. (2003), "Simulation of track–ground vibrations due to a high-speed train: the case of X-2000 at Ledsgard", *J. Sound Vib*., **261**(3), 503-526. https://doi.org/10.1016/S0022-460X(02)01007-6.

With, C., Bahrekazemi, M. and Bodare, A. (2006), "Validation of an empirical model for prediction of train-induced ground vibrations", *Soil Dyn. Earthq. Eng*., **26**(11), 983-990. https://doi.org/10.1016/j.soildyn.2006.03.005.

Xue, Y.G., Li, S.C., Zhang, D.F., Zhang, B. and Qiu, D.H. (2014), "Vibration characteristics in subway operation and environmental responses of ancient buildings", *Pol. J. Environ. Stud*., **23**(1), 231-241. https://doi.org/10.1016/j.ecolecon.2013.11.002.

Yin, Z.Z., Ding, J.M. and Shen, Y.K. (2008), "Analysis of building vibration and noise induced by metro", *Noise Vib. Control*, **28**(5), 147-150. https://doi.org/10.3724/SP.J.1005.2008.00527.

Zapfe, J.A. and Ungar, E.E. (2000), "Technical Note: A case study of potential ground-borne vibration reductions from targeted maintenance of subway cars", *Noise Control Eng. J*., **48**(5), 166-169. https://doi.org/10.3397/1.2827964.

Zhang, C.H. and Yang, X.J. (2011), "Transmission of ground vibration due to underground railway", *Environ. Eng*., **29**(2), 127-131. https://doi.org/10.1007/s12182-011-0123-3.

Zhu, Z.H., Davidson, M.T., Harik, I.E. and Wu, Y.Z. (2017), "Train-induced vibration characteristics of an integrated high-speed railway station", *J. Perform. Constr. Facil*., **31**(4), 1-14. https://doi.org/10.1061/(ASCE)CF.1943-5509.0001003.

Zou, C., Wang, Y.M. and Tao, Z.Y. (2020), "Train-induced building vibration and radiated noise by considering soil properties", *Sustain.*, **12**(3), 937. https://doi.org/10.3390/su12030937.

GC